



Molecular and microscopic characterisation of a novel pathogenic herpesvirus from Indian ringneck parrots (*Psittacula krameri*)

Michelle Sutherland^{a,*}, Subir Sarker^{b,c,**}, Shane R. Raidal^c

^a Burwood Bird and Animal Hospital, 128 Highbury Rd, Burwood, Vic, 3125, Australia

^b Department of Physiology, Anatomy and Microbiology, School of Life Sciences, La Trobe University, Bundoora, Vic, 3086, Australia

^c Veterinary Diagnostic Laboratory, Charles Sturt University, Wagga Wagga, NSW, 2678, Australia

ARTICLE INFO

Keywords:

Psittacine
Herpesvirus
Indian ringneck
Next-generation sequencing
Transmission electron microscopy

ABSTRACT

A high morbidity, high mortality disease process caused flock deaths in an Indian ringneck parrot (*Psittacula krameri*) aviary flock in Victoria, Australia. Affected birds were either found dead with no prior signs of illness, or showed clinical evidence of respiratory tract disease, with snicking, sneezing and dyspnoea present in affected birds. Necropsy examinations performed on representative birds, followed by cytological and histopathological examination, demonstrated lesions consistent with a herpesvirus bronchointerstitial pneumonia. Transmission electron microscopy analysis of lung tissue demonstrated typical herpesvirus virions measuring approximately 220 nm in diameter. Next generation sequencing of genomic DNA from lung tissue revealed a highly divergent novel Psittacid alphaherpesvirus of the genus *Iltovirus*. Iltoviruses have been previously reported to cause respiratory disease in a variety of avian species, but molecular characterisation of the viruses implicated has been lacking. This study presents the genome sequence of a novel avian herpesvirus species designated *Psittacid alphaherpesvirus-5* (PsHV-5), providing an insight into the evolutionary relationships of the alphaherpesviruses.

1. Introduction

The *Herpesviridae* are a diverse family of enveloped, double-stranded DNA viruses found in many different orders of vertebrates, including birds, reptiles, amphibians, fish and mammals (McGeoch and Davison, 1999). Herpesviruses have been further classified into the subfamilies that include alpha-, beta- and gammaherpesviruses. These classifications were initially based on the properties of the viruses described, with alphaherpesviruses associated with rapid viral replication, the ability to cause host cell lysis, and the capacity to establish latent infections (Lazic et al., 2008). However, phylogenetic relationships of herpesviruses are now formally based on their genetic characteristics, as defined by homology or nucleic acid sequences and the identification of particular genes that are unique to each subfamily (McGeoch and Davison, 1999). All currently available sequence data derived from avian herpesviruses have been consistent with the alphaherpesvirus subfamily (McGeoch and Davison, 1999; VanDevanter et al., 1996). Although alphaherpesviruses are fairly species specific, they typically exhibit a more variable host range compared to beta- or gamma-herpesviruses, and are able to establish latent infections in sensory ganglia (Roizman et al., 1992).

Of the nineteen known avian herpesviruses, alphaherpesviruses of the genus *Iltovirus* have been documented to cause respiratory disease. *Gallid alphaherpesvirus-1* (GaHV-1) causes infectious laryngotracheitis (ILT) in gallinaceous birds. This manifests as either a mild form associated with moderate mucoid tracheitis, conjunctivitis, and laryngeal and tracheal haemorrhage, or a severe form causing diphtheritic plaque formation in the larynx and trachea that may extend into the lungs and air sacs (Benton and Cover, 1958; Garcia et al., 2013).

In parrots, three alphaherpesviruses have been described; *Psittacid alphaherpesvirus-1* (PsHV-1; also known as Pacheco's Disease), PsHV-2, and PsHV-3. The viral genome of PsHV-1 consists of 163,025 base pairs (bp) (GenBank accession no. AY372243), and has been classified into four genotypes with distinct biological characteristics (Thureen and Keeler, 2006; Tomaszewski et al., 2003). *Psittacid alphaherpesvirus-2* and PsHV-1 are closely related viruses, and both have the ability to cause mucosal papilloma development, while PsHV-1 additionally causes an acute, rapidly fatal hepatic necrosis, or the insidious development bile duct and pancreatic duct neoplasms some months or years after initial infection. In addition, a herpesvirus with a tropism for the respiratory tract has been reported in various avian species, but confirmed by genetic sequencing only in Bourke's parrots (*Neopsophotus bourkii*) and

* Corresponding author. Present address: The Unusual Pet Vets, 210 Karingal Drive, Frankston, Vic, 3199, Australia.

** Corresponding author at: Department of Physiology, Anatomy and Microbiology, School of Life Sciences, La Trobe University, Bundoora, Vic, 3086, Australia.

E-mail addresses: michelle@unusualpetvets.com.au (M. Sutherland), s.sarker@latrobe.edu.au (S. Sarker), shraidal@csu.edu.au (S.R. Raidal).

eclectus parrots (*Eclectus roratus*) (Gabor et al., 2013; Shivaprasad and Phalen, 2012). Phylogenetic analysis of the virus affecting these species suggested a novel psittacid alphaherpesvirus in the genus *Iltovirus*, with the suggested name *Psittacid alphaherpesvirus-3* (PsHV-3) (Shivaprasad and Phalen, 2012). However, this nomenclature has yet to be ratified by the International Committee on Taxonomy of Viruses (ICTV, 2018). Typical histological lesions associated with PsHV-3 as reported in these species included the presence of intranuclear inclusion bodies within epithelial and syncytial cells of the trachea, bronchi, air capillaries and air sacs, with an absence of upper respiratory tract disease (Lazic et al., 2008; Raidal et al., 1995; Shivaprasad and Phalen, 2012). A viral respiratory infection with similar histopathological findings has also been described in Indian ringneck parrots (*Psittacula krameri*), Amazon parrots (*Amazona* spp.), cockatiels (*Nymphicus hollandicus*) eastern rosellas (*Platycercus eximus*) and princess parrots (*Polytelis alexandrae*) (Lazic et al., 2008; Tsai et al., 1993). However, in these reports, phylogenetic analyses of the implicated virus were not performed, so while it has been supposed that PsHV-3 was the causative agent based on similarities in clinical findings and histopathology, a definitive aetiological diagnosis should not be assumed in these cases. Phylogenetic analysis has shown that *Psittacid alphaherpesvirus-3* is more closely related to GaHV-1 and *Passerid herpesvirus-1*, a virus causing tracheitis and bronchitis in Gouldian finches (*Erythrura gouldiae*) (Wellehan et al., 2003), than PsHV-1 or PsHV-2. Additionally, *Magellanic penguin herpesvirus-1* (MagHV-1) has been associated with an outbreak of high mortality respiratory disease in Magellanic penguins (*Spheniscus magellanicus*) in a rehabilitation facility (Niemeyer et al., 2017). Phylogenetic analyses grouped this virus with *Gaviid herpesvirus-1* (GavHV-1), a virus associated with respiratory disease in common loons (*Gavia immer*) (Niemeyer et al., 2017; Quesada et al., 2011).

The aims of this study were to report the clinical, pathological and microscopic findings associated with a novel herpesvirus causing disease in Indian ringneck parrots (*P. krameri*) in Australia, as well as to sequence and analyse its draft genome, with particular attention to the novel genomic features of this virus.

2. Materials and methods

2.1. Sample history and collection

A high morbidity/mortality disease process caused flock deaths in an aviary flock of Indian ringneck parrots in Victoria, Australia during the breeding season. All age groups were affected. Two representative birds (one juvenile, one adult) were presented for post-mortem examination. Heart and lung tissue were submitted to an external laboratory (IDEXX Laboratories, Glen Waverley, Victoria, Australia) for bacterial culture and microbial sensitivity testing.

2.2. Cytology and histopathological examination of the tissues

Impression smears of lung, liver and renal tissue were made, and stained with Wright's-Giemsa stain. Fresh tissue samples were taken from the lung, liver and kidney and stored frozen at -18°C . Visceral organs and brain tissue were fixed in 10% buffered formalin and were submitted to the Veterinary Diagnostic Laboratory, Charles Sturt University, Wagga Wagga, Australia, for histopathological examination, along with the impression smears for cytology. The formalin-fixed tissues were embedded in paraffin, sectioned at $4\mu\text{m}$, and stained with haematoxylin and eosin.

2.3. Transmission electron microscopy

Lung tissue from affected birds was suspended in 1:10 phosphate buffered saline (PBS), followed by grinding with a sterile round glass body homogeniser. Suspensions were clarified by centrifugation at 14,000 g for 5 min, followed by filtration of the supernatant through a

0.45 μm filter. The filtrate was then adsorbed onto a 400-mesh copper EM grid coated with a thin film of carbon for 5 min. Excess solution was removed using 3 MM filter paper (Whatman) and the grid rinsed briefly with distilled water before negative staining with three 10 s applications of 2% [w/v] uranyl acetate (Electron Microscopy Sciences, PA, USA) followed by removal of excess stain on filter paper after each application. Grids were air-dried for 20 min before imaging on a JEOL JEM-2100 transmission electron microscope as previously described (Sarker et al., 2017a, 2018).

2.4. DNA extraction, library construction, and sequencing

Based on the suspicion that the herpesvirus inclusions seen on histopathology in this case may be caused by the same herpesvirus as previously described in Indian ringnecks, (Helfer et al., 1980; Lazic et al., 2008; Tsai et al., 1993) an attempt to determine the genome sequence of the virus was undertaken.

Collected lung tissue was aseptically dissected and mechanically homogenised in lysis buffer using disposable tissue grinder pestles, then transferred into a 1.5 mL microcentrifuge tube (Eppendorf). Total genomic DNA was isolated according to established methods (Sarker et al., 2018) using a ReliaPrep gDNA Tissue Miniprep System (Promega, USA). The Illumina Nextera XT DNA Library Prep V3 Kit was used for quantification and quality assessment of the extracted DNA, followed by library preparation according to our published protocol (Sarker et al., 2018, 2017b). The quality and quantity of the prepared library was assessed using an Agilent Tape Station (Agilent Technologies) under the La Trobe University Genomics Platform. The prepared library was normalised and pooled in equimolar quantity. The quality and quantity of the final pooled library was further assessed as described above before sequencing by the facility. Cluster generation and sequencing of the pooled DNA-library was sequenced as paired-end on Illumina® MiSeq chemistry according to the manufacturer's instructions.

2.5. Assembly protocol and genome annotations

Sequencing data was analysed according to a previously established pipeline (Sarker et al., 2017a, b) using Geneious (version 10.2.2, Biomatters, New Zealand), and CLC Genomics Workbench 9.5.4. A total of over 7.2 million MiSeq reads with an average read length of approximately over 185 bp was used to obtain the draft genome of *Psittacid alphaherpesvirus-5* (PsHV-5). Preliminary quality evaluation for all raw reads was generated, pre-processed to remove ambiguous base calls and poor-quality reads, and Illumina adapter trimming. Trimmed sequence reads were filtered against a bird genome (*Apteryx australis mantelli*, GenBank accession number LK064674) to remove host DNA sequence reads. Unmapped reads were used as input data for *de novo* assembly using SPAdes assembler (version 3.10.0) (Bankevich et al., 2012) in Geneious. This yielded a single contig of 120,899 bp length.

The assembled draft genome of PsHV-5 was first annotated using the Genome Annotation Transfer Utility (GATU) (Tcherepanov et al., 2006) with PsHV-1 (GenBank accession no. AY372243) as the reference genome and further verification of the predicted open reading frames (ORFs) were performed using Geneious (version 10.2.2). Open reading frames longer than 50 amino acids with minimal overlapping (overlaps not exceeding 25% of one of the genes) to other ORFs were selected and annotated. These ORFs were subsequently extracted into a FASTA file, and similarity searches including nucleotide (BLASTx) and protein (BLASTp) were performed on annotated ORFs as potential genes if they shared significant sequence similarity to known viral or cellular genes (BLAST E value $\leq e^{-4}$) or contained a putative conserved domain as predicted by BLASTp (Benson et al., 2013). Additionally, searches for conserved secondary structure (HHpred) (Zimmermann et al., 2018) and protein homologs (Phyre2) (Kelley et al., 2015) were used to help predict the function of possible unique ORFs predicted in this study.

2.6. Phylogenetic analyses

The translated amino acid sequence of the DNA polymerase gene of the PsHV-5 was extracted, and aligned with other representative herpesvirus sequences using MAFFT (version 7.388) (Kato and Standley, 2013) under BLOSUM62 scoring matrix in Geneious (version 10.2.2). A maximum likelihood phylogenetic tree was constructed using a Le Gascuel (LG) substitution model, and 1000 bootstrap resamplings were chosen to generate the tree using tools available in Geneious (version 10.2.2). To investigate the evolutionary relationship among available herpesvirus DNA sequences more closely, partial nucleotide sequences of DNA polymerase genes were selected, and aligned with MAFFT (version 7.388) (Kato and Standley, 2013) in Geneious (version 10.2.2). A maximum likelihood phylogenetic tree was constructed using a HKY85 substitution model, and 1000 bootstrap resamplings were chosen to generate tree using tools available in Geneious (version 10.2.2) (Guindon et al., 2010).

3. Results

3.1. Outbreak details

All age groups of Indian ringneck parrots in the aviary were affected. The aviary contained approximately 300 birds, consisting of 160 breeding adults (80 pairs), 115 chicks and around 25 non-breeding birds. One hundred and twenty adult birds (116 breeding adults) and 80 chicks were affected, giving a morbidity rate of 75% in adults and 69.5% in chicks. The clinical presentation was acute fatality in 85 adults (70% affected birds; all breeding adult) and 60 (75%) of affected chicks. The owner reported affected birds were either found dead with no prior signs of illness, or showed evidence of respiratory disease with signs including inspiratory dyspnoea, stridor, and mucus in the upper respiratory tract.

3.2. Gross necropsy findings

On gross necropsy, lesions included pericardial haemorrhage and pericardial sac distension; left atrial enlargement; diffuse consolidation, congestion and red discolouration of the lungs; thickened air sacs with cream/yellow discolouration, and pale kidneys.

3.3. Microbiology

There was no bacterial growth from heart or lung tissue under aerobic or anaerobic conditions.

3.4. Histopathological findings

Cytological examination of the lung impression smears revealed large numbers of syncytia, some containing 20–30 nuclei, ballooning

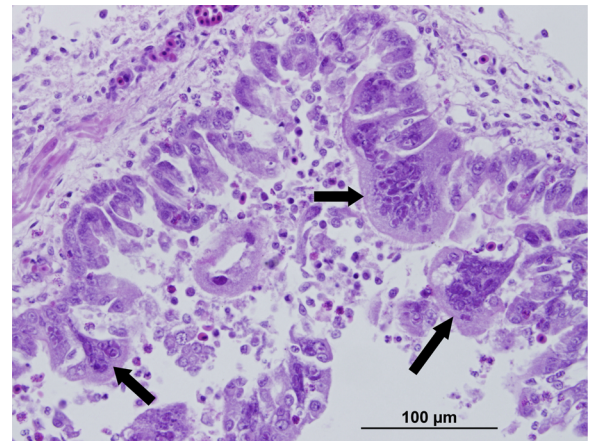


Fig. 2. Histopathological section of lung tissue from an Indian ringneck parrot infected with a novel herpesvirus causing bronchointerstitial pneumonia. Multiple syncytia (arrows) are evident within the epithelium and lining of a parabronchus. Diffuse oedema is present in the submucosa with a mixed inflammatory infiltrate and exudate into the lumen. Haematoxylin and eosin. Bar = 100 µm.

degeneration of nuclei, and margined chromatin (Fig. 1). A moderate number of heterophils and macrophages were also present. Impression smears of the liver and kidney appeared normal (data not shown).

On histopathological examination, samples from both birds demonstrated extensive acute inflammation of the bronchi and parabronchi with haemorrhage, exudating heterophils and focal epithelial necrosis associated with epithelial syncytia and eosinophilic intranuclear inclusions consistent with herpesvirus infection (Fig. 2). In the adult bird, this was associated with large numbers of coccoid bacteria (suspected to be a *Staphylococcus* spp.). In the chick, the viral inclusions and inflammation extended into the adjacent air sacs and parietal pericardium with diffuse perivascular haemorrhage and oedema associated with the attached air sac inflammation. Changes in other organs included diffuse moderate to marked congestion. A histopathological diagnosis of herpesvirus bronchointerstitial pneumonia and severe acute heterophilic airsacculitis was made.

3.5. Electron microscopic findings

Transmission electron microscopy (TEM) analysis of negatively stained lung tissue material sourced from a captive Indian ringneck parrot showed typical herpesvirus virions measuring approximately 220 nm in diameter. The virions comprised naked nucleocapsids rimmed by hollow capsomers (Fig. 3).

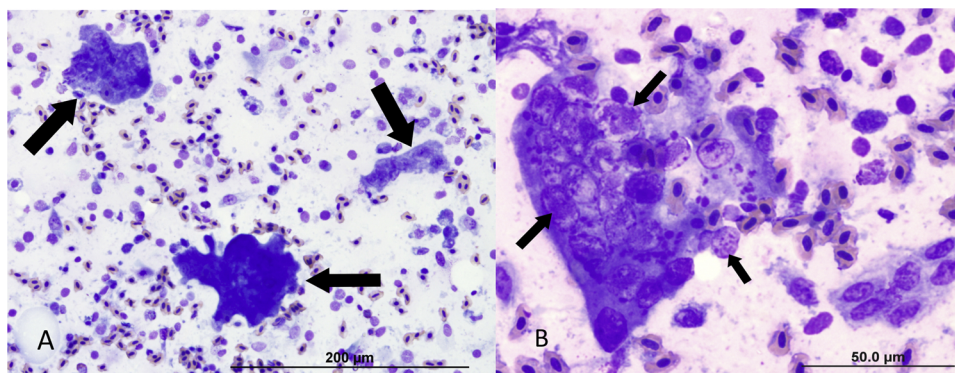


Fig. 1. Impression smears of lung tissue from an Indian ringneck parrot infected with a herpesvirus bronchointerstitial pneumonia. A. Three relatively large syncytia (arrows). Bar = 200 µm. Wright's Giemsa stain. B. Numerous nuclei containing intranuclear inclusions within a syncytium (arrows). Bar = 50 µm. Wright's Giemsa stain.

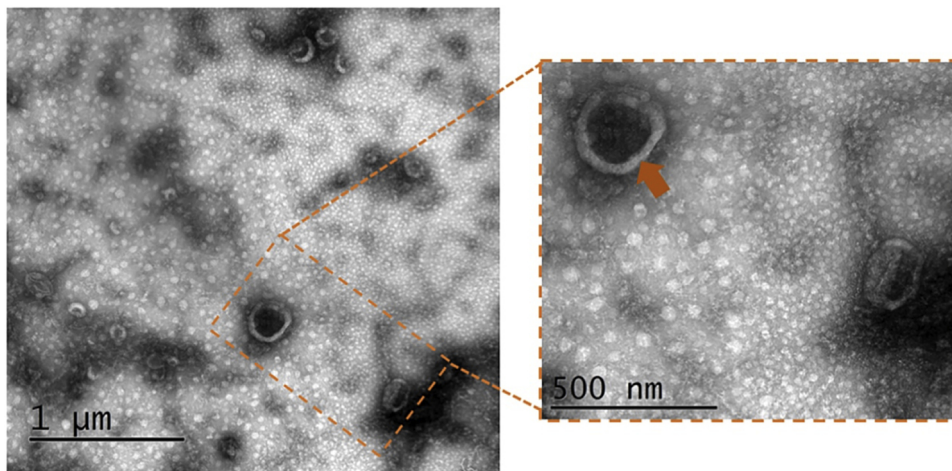


Fig. 3. Transmission electron microscopic analysis of negatively stained lung tissues from an Indian ringneck parrot. Virus particles showing typical herpesvirus virions (orange arrow).

3.6. Genomic structure and comparative analyses of PsHV-5

The assembled *Psittacid alphaherpesvirus-5* (PsHV-5) draft genome was a linear double-stranded DNA molecule of 120,899 bp in length, excluding terminal repeats, and has been deposited in GenBank under the accession number [MK955929](#). Like most avian herpesviruses, the PsHV-5 draft genome contained 81 predicted methionine-initiated ORF encoding proteins and was numbered from left to right (Table 1). The protein sequences encoded by the predicted ORFs were compared to the sequences in the non-redundant protein sequence database at the National Center for Biotechnology Information (NIH, Bethesda, MD) using BLASTP identified homologs with significant protein sequence similarity (E value $\leq e^{-4}$) for 59 genes belonging to herpesviruses (Table 1). In addition, an ORF encoded by PsHV-5 (ORF002) demonstrated a significant protein homolog (67.3% confidence on 53% query protein sequence) with vesicular stomatitis virus matrix protein. Interestingly, PsHV-5 contained 21 predicted protein-coding genes that were not present in any other herpesvirus, nor did they match any sequences in the NR protein database using BLASTP and BLASTx; these unique ORFs encoded proteins of 54 to 375 amino acids in length (Table 1). Furthermore, these unique protein-coding genes did not show any significant homology with known proteins using HHpred and Phyre2 searches.

Among the predicted protein-coding genes of the PsHV-5 genome, the highest number of protein-coding genes (33) demonstrated homologs to the isolated *Gallid alphaherpesvirus-1*, followed by *Psittacid alphaherpesvirus-1* (20), *Sphenicid alphaherpesvirus-1* (2), and one of each gene of *Anatid alphaherpesvirus-1*, *Columbid alphaherpesvirus-1*, *Falconid herpesvirus-1* and *Equid alphaherpesvirus-4* (Table 1). All conserved genes of PsHV-5 showed the amino acid sequence similarity ranges from 22.8 to 71.34 to orthologs of the other herpesvirus sequences.

Comparison of the PsHV-5 draft genome to other avian herpesvirus genomes showed the central region to be relatively conserved in gene content (Table 1). In comparison to PsHV-1, eight conserved genes such as VP11-12 (UL46), membrane protein (UL45) virion host shut-off (UL41), putative membrane protein (UL43), myristylated tegument protein (UL11), protein kinase (US2), glycoprotein G (US4) and regulatory protein (ICP4B) were missing in the PsHV-5 genome.

3.7. Evolutionary relationships of PsHV-5

To track the evolutionary pathway of the newly discovered PsHV-5, phylogenetic analyses were conducted with the inclusion of other selected herpesviruses of complete DNA polymerase gene. In the resulting maximum likelihood phylogenetic tree, PsHV-5 was positioned in a distinct sub-clade (bootstrap support 100%) with a clade dominated by all other avian herpesvirus sequences such as *Cacatuid alphaherpesvirus-2* (CaHV-2), PsHV-1

and GaHV-1 (Fig. 4). In agreement with phylogenetic relationships, the PsHV-5 DNA polymerase gene sequence also demonstrated relatively lower identities with CaHV-2 (51.3%), PsHV-1 (52.8%) and GaHV-1 (52.0%).

To better understand these evolutionary relationships within avian herpesviruses, the partial nucleotide sequences of the DNA polymerase gene were utilised to construct a phylogenetic tree. A well-supported distinct sub-clade (100%) was generated by PsHV-5 and placed between PsHV-3, GavHV-1 and GaHV-1 (Fig. 5). This scenario was consistent with that identified by the pairwise nucleotide comparison of the partial DNA polymerase gene among selected avian herpesvirus sequences in this study, demonstrating the highest nucleotide identity with PsHV-3 (99.8%), followed by GavHV-1 (59.0%), and GaHV-1 (58.7%).

4. Discussion

This paper presents the detection and characterisation of a highly divergent novel pathogenic PsHV-5 directly from naturally occurring herpesvirus infection in Indian ringneck parrots. Disease caused by herpesvirus infection in this species has been reported previously; (Lazic et al., 2008) however, there is an absence of genome scale sequence data for previously described herpesvirus infections in *P. krameri*, and an unclear evolutionary history with other members of the *Herpesviridae*. In the present study, the sequenced PsHV-5 genome architecture was consistent with other psittacid herpesvirus genomes in terms of gene content; however, it was distinct from other herpesviruses in multiple ways. Overall, the DNA polymerase protein-coding sequence of PsHV-5 was significantly different to other described herpesviruses, demonstrating relatively low identities with PsHV-1 and GaHV-1 (52.8% and 52.0%, respectively). The novel PsHV-5 was missing eight conserved genes compared to PsHV-1, and contains 21 predicted genes that are not found in any other herpesvirus. However, considering the presence of numerous hypothetical and or unique genes in the PsHV-5 genome, it is possible that the genes encoding these functions are present but were not identified due to sequence divergence. Hence, PsHV-5 is genetically sufficiently different to be considered a separate virus species in the genus *Iltovirus*.

The main findings at necropsy in this case were diffuse consolidation, congestion and red discolouration of the lungs; thickened air sacs with cream/yellow discolouration; pericardial haemorrhage and pericardial sac distension; left atrial enlargement; and pale kidneys. These findings are similar to previously described lesions associated with a herpesvirus affecting parakeets with a tropism for the lower respiratory tract (Lazic et al., 2008; Raidal et al., 1995; Shivaprasad and Phalen, 2012; Tsai et al., 1993). Cytology alongside histopathology confirmed the presence of a herpesvirus bronchointerstitial pneumonia and air sacculitis.

Table 1
Predicted protein-coding genes of PsHV-5.

PsHV5 synteny	Position	Nt Length	AA length	PsHV1 synteny	Best hit (PI/e-value/%identity/organism)	product
001	151-429	279	92		no significant BLASTP hits	hypothetical protein
002*	1841-2029	189	62		53% (33 residues) have been modelled with 67.3% confidence	vesicular stomatitis virus matrix protein
003	2036-2263	228	75		no significant BLASTP hits	hypothetical protein
004	3495-5144	1650	549		AER28030.1/7.00E-14/30.77/Gallid alphaherpesvirus 1	protein IF
005	6681-5224	1458	485	UL54	AUT11937.1/1.00E-69/36.16/Gallid alphaherpesvirus 1	multifunctional expression regulator
006	6990-7541	552	183	ORFG	YP_001285929.1/2.00E-19/46.51/Psittacid alphaherpesvirus 1	protein IG
007	8615-7569	1047	348	UL53	SCL76916.1/4.00E-25/23.93/Sphenicid alphaherpesvirus 1	envelope glycoprotein K
008	11833-8546	3288	1095	UL52	AGN48237.1/0.00E+00/35.46/Gallid alphaherpesvirus 1	helicase-primase primase subunit
009	11766-12338	573	190	UL51	NP_944383.1/5.00E-48/50.35/Psittacid alphaherpesvirus 1	tegument protein
010	12974-12417	558	185	UL50	YP_003084369.1/1.00E-16/32.95/Anatid alphaherpesvirus 1	dUTPase
011	13417-13217	201	66		no significant BLASTP hits	hypothetical protein
012	14276-14986	711	236	UL49	NP_944386.1/5.00E-24/39.68/Psittacid alphaherpesvirus 1	tegument protein VP22
013	15098-16654	1557	518	UL48	AER28038.1/2.00E-69/34.49/Gallid alphaherpesvirus 1	transactivating tegument protein VP16
014	18407-19456	1050	349		AGC23047.1/3.00E-06/30.41/Gallid alphaherpesvirus 1	hypothetical protein
015	21994-19703	2292	763	UL22	AGF43577.1/3.00E-84/26.82/Gallid alphaherpesvirus 1	glycoprotein H
016	23264-22149	1116	371	UL23	NP_944395.1/7.00E-64/35.21/Psittacid alphaherpesvirus 1	thymidine kinase
017	23141-24004	864	287	UL24	AGN48252.1/2.00E-28/36.04/Gallid alphaherpesvirus 1	nuclear protein
018	24110-25831	1722	573	UL25	AEB97316.1/3.00E-161/45.07/Gallid alphaherpesvirus 1	DNA packaging tegument protein
019	26006-27811	1806	601	UL26	AFD36724.1/1.00E-68/32.95/Gallid alphaherpesvirus 1	capsid maturation protease
020	30525-27901	2625	874	UL27	ABX59521.1/0.00E+00/53.55/Gallid alphaherpesvirus 1	envelope glycoprotein B
021	32840-30558	2283	760	UL28	NP_944401.1/0.00E+00/45.62/Psittacid alphaherpesvirus 1	DNA packaging terminase subunit 2
022	36482-32916	3567	1188	UL29	AGN48180.1/0.00E+00/48.54/Gallid alphaherpesvirus 1	single-stranded DNA-binding protein
023	36742-40107	3366	1121	UL30	NP_944403.1/0.00E+00/54.17/Psittacid alphaherpesvirus 1	DNA polymerase catalytic subunit
024	41065-40070	996	331	UL31	NP_944404.1/2.00E-109/56.14/Psittacid alphaherpesvirus 1	nuclear egress lamina protein
025	42812-41058	1755	584	UL32	YP_182361.1/7.00E-177/43.79/Psittacid alphaherpesvirus 1	DNA packaging protein
026	42811-43212	402	133	UL33	YP_182362.1/5.00E-28/50.00/Gallid alphaherpesvirus 1	DNA packaging protein
027	43315-44136	822	273	UL34	NP_944407.1/4.00E-52/45.98/Psittacid alphaherpesvirus 1	nuclear egress membrane protein
028	44151-44684	534	177	UL35	YP_182364.1/1.00E-17/48.39/Gallid alphaherpesvirus 1	small capsid protein
029	50938-44735	6204	2067	UL36	YP_182365.1/3.00E-159/28.07/Gallid alphaherpesvirus 1	large tegument protein
030	54012-51007	3006	1001	UL37	AFD36499.1/2.00E-48/22.91/Gallid alphaherpesvirus 1	tegument protein
031	54176-55558	1383	460	UL38	AGN48189.1/1.00E-65/34.99/Gallid alphaherpesvirus 1	capsid triplex subunit 1
032	55811-58174	2364	787	UL39	ATG31558.1/0.00E+00/51.28/Gallid alphaherpesvirus 1	ribonucleotide reductase subunit 1
033	58197-59135	939	312	UL40	AEB97332.1/4.00E-165/71.34/Gallid alphaherpesvirus 1	ribonucleotide reductase subunit 2
034	59325-60440	1116	371	UL42	NP_944415.1/2.00E-33/28.83/Psittacid alphaherpesvirus 1	DNA polymerase processivity factor
035	60824-60639	186	61		no significant BLASTP hits	hypothetical protein
036	62040-63287	1248	415	UL44	NP_944417.1/2.00E-13/22.80/Psittacid alphaherpesvirus 1	envelope glycoprotein C
037	65057-63441	1617	538	UL21	AGN48196.1/9.00E-17/24.67/Gallid alphaherpesvirus 1	tegument protein
038	65244-65963	720	239	UL20	AGC23075.1/3.00E-08/24.88/Gallid alphaherpesvirus 1	envelope protein
039	66184-70392	4209	1402	UL19	ATG31660.1/0.00E+00/55.52/Gallid alphaherpesvirus 1	major capsid protein
040	70664-71617	954	317	UL18	YP_182377.1/4.00E-106/45.85/Gallid alphaherpesvirus 1	capsid triplex subunit 2
041	72944-71688	1257	418	UL15a	Q6UD12.1/0/65.54/Psittacid alphaherpesvirus 1	tripartite terminase subunit 3
042	72879-75110	2232	743	UL17	AER28075.1/2.00E-80/28.84/Gallid alphaherpesvirus 1	DNA packaging tegument protein
043	75047-76078	1032	343	UL16	BAV93254.1/4.00E-43/30.67/Equid alphaherpesvirus 4	tegument protein
044	77296-76127	1170	389	UL15b	AGC23078.1/5.00E-93/46.55/Gallid alphaherpesvirus 1	DNA packaging terminase subunit 1
045	77295-77885	591	196	UL14	NP_944426.1/3.00E-18/35.29/Psittacid alphaherpesvirus 1	tegument protein
046	77999-79123	1125	374	UL13	NP_944427.1/1.00E-48/32.56/Psittacid alphaherpesvirus 1	tegument serine/threonine protein kinase
047	79120-80598	1479	492	UL12	ATG31573.1/9.00E-114/39.87/Gallid alphaherpesvirus 1	deoxyribonuclease
048	82122-80833	1290	429	UL10	NP_944430.1/5.00E-64/29.81/Psittacid alphaherpesvirus 1	envelope glycoprotein M
049	82133-84841	2709	902	UL9	NP_944431.1/0.00E+00/43.59/Psittacid alphaherpesvirus 1	DNA replication origin-binding helicase
050	84934-87123	2190	729	UL8	AGC23167.1/2.00E-68/27.60/Gallid alphaherpesvirus 1	helicase primase subunit
051	88033-87161	873	290	UL7	NP_944433.1/3.00E-53/37.54/Psittacid alphaherpesvirus 1	tegument protein
052	90168-88030	2139	712	UL6	NP_944434.1/5.00E-169/44.16/Psittacid alphaherpesvirus 1	capsid portal protein
053	90325-92892	2568	855	UL5	NP_944435.1/0.00E+00/51.68/Psittacid alphaherpesvirus 1	helicase-primase helicase subunit
054	93030-93572	543	180	UL4	YP_182391.1/3.00E-43/43.26/Gallid alphaherpesvirus 1	nuclear protein
055	93951-93616	336	111		no significant BLASTP hits	hypothetical protein
056	94588-93956	633	210	UL3	NP_944437.2/2.00E-52/63.31/Psittacid alphaherpesvirus 1	nuclear protein
057	95698-94787	912	303	UL2	AER28089.1/5.00E-77/50.62/Gallid alphaherpesvirus 1	uracil-DNA glycosylase
058	96128-95688	441	146	UL1	CAA65896.1/4.00E-09/35.11/Gallid alphaherpesvirus 1	envelope glycoprotein L
059	97269-96217	1053	350		no significant BLASTP hits	hypothetical protein
060	97774-97610	165	54		no significant BLASTP hits	hypothetical protein
061	97741-97917	177	58		no significant BLASTP hits	hypothetical protein
062	101308-98054	3255	1084	ICP4	ADK89102.1/3.00E-31/40.27/Gallid alphaherpesvirus 1	regulatory protein
063	101276-101596	321	106		no significant BLASTP hits	hypothetical protein
064	101849-101586	264	87		no significant BLASTP hits	hypothetical protein
065	102276-102557	282	93		no significant BLASTP hits	hypothetical protein
066	102972-102739	234	77		no significant BLASTP hits	hypothetical protein
067	102987-103301	315	104		no significant BLASTP hits	hypothetical protein
068	104260-105177	918	305		no significant BLASTP hits	hypothetical protein
069	107174-105630	1545	514	US8	SCL76990.1/3.00E-13/23.88/Sphenicid alphaherpesvirus 1	envelope glycoprotein E
070	108433-107357	1077	358	US7	AGC23103.1/4.00E-16/26.26/Gallid alphaherpesvirus 1	envelope glycoprotein I
071	109461-108547	915	304	US6	YP_009353003.1/1.00E-06/23.53/Columbid alphaherpesvirus 1	envelope glycoprotein D
072	110426-109554	873	290	US6	YP_009046593.1/1.00E-07/26.98/Falconid herpesvirus 1	envelope glycoprotein D

(continued on next page)

affecting the respiratory system in Australia (90–120 nm diameter) (Gabor et al., 2013). There are numerous virus species classified as *Herpesviridae* that infect a range of vertebrates and invertebrates, and the virion size of these viruses is variable, ranging from 120 to 230 nm diameter (Gibson, 1996). Interspecific differences in virion size between avian herpesviruses cannot be ruled out; however, the variability of virion size between previously described avian herpesviruses and the one identified in this study provides additional support for the herpesvirus identified in this study being a novel virus.

The genome sequencing of a novel herpesvirus from infected lung tissue confirmed the presence of a novel PsHV that is most closely related to, but genetically divergent from PsHV-3, and distantly related to other avian herpesviruses according to phylogenetic tree analysis (Figs. 4 and 5).

Based on the similarity of lesions demonstrated on histopathology, we suggest that the virus characterised in this case may be similar to previously reported respiratory herpesvirus in Indian ringneck parrots (Lazic et al., 2008; Tsai et al., 1993) that had a demonstrated tropism for the lung and lower respiratory tract tissues. Such lesions have previously been identified on tissue histopathology and electron microscopy, but molecular characterization has been lacking.

The phylogenetic tree derived from amino acid sequences of the DNA polymerase gene shows that the sub-clade consisting of *Cacatuūid alphaherpesvirus-1* (CaHV-1), GaHV-1, and psittacid herpesviruses is well supported and segregated into four well-supported monophyletic sub-clades (Fig. 4). As this figure shows, it is evident that PsHV-5 is most closely related to PsHV-1, GaHV-1 and CaHV-2, inferring that these viruses originated from a common ancestor. In addition, the partial nucleotide sequences of the DNA polymerase gene of the novel PsHV-5 compared to other selected avian herpesviruses demonstrated the highest nucleotide identity with PsHV-3, GavHV-1 and GaHV-1, respectively (Fig. 5). These findings infer that PsHV-5 may be more closely related at a conserved gene level than across the whole genome, and highlights the value of complete genome characterisation.

5. Conclusions

This study presents the genome sequence of a novel avian herpesvirus that caused a high morbidity, high mortality outbreak of lower respiratory tract disease in an Indian ringneck aviary in Australia. It also provides an insight into the evolutionary relationships of this virus with other related herpesviruses, including PsHV-3, that has also been documented to cause respiratory disease in parrots both in Australia and globally. The PsHV-5 genome has enhanced the genomic information available for the *Iltovirus* genus and will contribute to our understanding of avian herpesviruses more generally. Together with sequence similarities from PsHV-5 and other avian herpesviruses, this study concluded that the PsHV-5 complete genome from Indian ring-necks in Victoria, Australia, described here, is sufficiently diverse compared to other previously described avian herpesviruses and that it should be considered a separate species. Genomic identification of avian herpesviruses is essential to the understanding of their epizootiology, and is applicable to our knowledge of appropriate management of disease outbreaks in individual birds and aviaries, biosecurity aspects relating to the international trade of birds, and conservation efforts of vulnerable avian species (Shivaprasad and Phalen, 2012).

Acknowledgements

The authors would like to thank the AAVAC Research Fund for providing funding towards the costs of the genomic sequencing. The authors also gratefully acknowledge the Latrobe Institute for Molecular Science (LIMS) Bioimaging Facility for the use of the Transmission Electron Microscope.

Appendix A. Supplementary data

Supplementary material related to this article can be found, in the online version, at doi:<https://doi.org/10.1016/j.vetmic.2019.108428>.

References

- Bankevich, A., Nurk, S., Antipov, D., Gurevich, A.A., Dvorkin, M., Kulikov, A.S., Lesin, V.M., Nikolenko, S.I., Pham, S., Pribelski, A.D., Pyshkin, A.V., Sirotkin, A.V., Vyahhi, N., Tesler, G., Alekseyev, M.A., Pevzner, P.A., 2012. SPAdes: a new genome assembly algorithm and its applications to single-cell sequencing. *J. Comput. Biol.* 19, 455–477. <https://doi.org/10.1089/cmb.2012.0021>.
- Benson, D.A., Cavanaugh, M., Clark, K., Karsch-Mizrachi, I., Lipman, D.J., Ostell, J., Sayers, E.W., 2013. GenBank. *Nucleic Acids Res.* 41, D36–42.
- Benton, M.S., Cover, W.J., 1958. The biological variation of the infectious laryngotracheitis virus. *Avian Dis.* 2, 375–383.
- Gabor, M., Gabor, L.J., Peacock, L., Srivastava, M., Rosenwax, A., Phalen, D., 2013. Psittacid herpesvirus-3 infection in the eclectus parrot (*Eclectus roratus*) in Australia. *Vet. Pathol.* 50, 1053–1057. <https://doi.org/10.1177/0300985813490753>.
- Garcia, M., Spatz, S., Guy, J.S., 2013. Infectious laryngotracheitis. In: Swain, D.E., Glisson, J.R., McDougald, L.R., Nolan, L.K., Suarez, D.L. (Eds.), *Diseases of Poultry*. John Wiley and Sons Inc., Hoboken, NJ, pp. 161–180.
- Gibson, W., 1996. Structure and assembly of the virion. *Intervirology* 39, 389–400.
- Guindon, S., Dufayard, J.-F., Lefort, V., Anisimova, M., Hordijk, W., Gascuel, O., 2010. New algorithms and methods to estimate maximum-likelihood phylogenies: assessing the performance of PhyML 3.0. *Syst. Biol.* 59, 307–321. <https://doi.org/10.1093/sysbio/syq010>.
- Helffer, D.H., Schmitz, J.A., Seefeldt, S.L., Lowenstein, L., 1980. A new viral respiratory infection in parakeets. *Avian Dis.* 24, 781–783.
- ICTV, 2018. International Committee on Taxonomy of Viruses (ICTV). Accessed 15 September 2019. <https://talk.ictvonline.org/taxonomy/>.
- Katoh, K., Standley, D.M., 2013. MAFFT multiple sequence alignment software version 7: improvements in performance and usability. *Mol. Biol. Evol.* 30, 772–780. <https://doi.org/10.1093/molbev/mst010>.
- Kelley, L.A., Mezulis, S., Yates, C.M., Wass, M.N., Sternberg, M.J.E., 2015. The Phyre2 web portal for protein modeling, prediction and analysis. *Nat. Protoc.* 10, 845.
- Lazic, T.W., Ackerman, M.R., Drahos, J.M., Stasko, J., Haynes, J.S., 2008. Respiratory herpesvirus infection in two Indian Ringneck parakeets. *J. Vet. Diagn. Invest.* 20, 235–238. <https://doi.org/10.1177/104063870802000217>.
- McGeoch, D.J., Davison, A.J., 1999. The molecular evolutionary history of the herpesviruses. In: Domingo, E., Webster, R., Holland, J. (Eds.), *Origin and Evolution of Viruses*. Academic Press, San Diego, pp. 441–465.
- Niemeyer, C., Favero, C.M., Shivaprasad, H.L., Uhart, M., Musso, C.M., Rago, M.V., Silva Filho, R.P., Canabarro, P.L., Craig, M.L., Olivera, V., Pereda, A., Brandão, P.E., Catão-Dias, J.L., 2017. Genetically diverse herpesviruses in South American Atlantic coast seabirds. *PLoS One* 12, e0178811. <https://doi.org/10.1371/journal.pone.0178811>.
- Quesada, R., Heard, D.J., Aitken-Palmer, C., Hall, N., Conley, K.J., Childress, A.L., Wellehan, J.F., 2011. Detection and phylogenetic characterization of a novel herpesvirus from the trachea of two stranded Common Loons (*Gavia immer*). *J. Wildl. Dis.* 47, 233–239.
- Raidal, S.R., Gill, J.H., Cross, G.M., 1995. An acute respiratory disease with inclusion body bronchitis and splenitis in Bourke's parrots. *Aust. Vet. Pract.* 25, 170–171.
- Roizman, B., Desrosiers, R.C., Fleckenstein, B., Lopez, C., Minson, A.C., Studdert, M.J., 1992. The family Herpesviridae: an update. *Arch. Virol.* 123, 425–449.
- Sarker, S., Das, S., Lavers, J.L., Hutton, I., Helbig, K., Imbrey, J., Upton, C., Raidal, S.R., 2017a. Genomic characterization of two novel pathogenic avipoxviruses isolated from pacific shearwaters (*Ardenna* spp.). *BMC Genomics* 18, 298.
- Sarker, S., Isberg, S.R., Milic, N.L., Lock, P., Helbig, K.J., 2018. Molecular characterization of the first saltwater crocodilepox virus genome sequences from the world's largest living member of the Crocodylia. *Sci. Rep.* 8, 5623.
- Sarker, S., Roberts, H.K., Tidd, N., Ault, S., Ladmore, G., Peters, A., Forwood, J.K., Helbig, K., Raidal, S.R., 2017b. Molecular and microscopic characterization of a novel Eastern grey kangarooopox virus genome directly from a clinical sample. *Sci. Rep.* 7, 16472.
- Shivaprasad, H.L., Phalen, D.N., 2012. A novel herpesvirus associated with respiratory disease in Bourke's parrots. *Avian Pathol.* 41, 531–539.
- Tcherepanov, V., Ehlers, A., Upton, C., 2006. Genome Annotation Transfer Utility (GATU): rapid annotation of viral genomes using a closely related reference genome. *BMC Genomics* 7, 1–10.
- Thureen, D.R., Keeler, C.L., 2006. Psittacid herpesvirus 1 and infectious laryngotracheitis virus: comparative genome sequence analysis of two avian alphaherpesviruses. *J. Virol.* 80, 7863–7872.
- Tomaszewski, E., Kaleta, E.F., Phalen, D.N., 2003. Molecular phylogeny of the psittacid herpesviruses causing Pacheco's disease: correlation of genotype with phenotypic expression. *J. Virol.* 77, 11260–11267.
- Tsai, S.S., Hirai, K., Itakura, C., 1993. Herpesvirus infection in psittacine birds in Japan. *Avian Pathol.* 22, 141–156.
- VanDevanter, D.R., Warren, P., Bennett, L., Schultz, E.R., Coulter, S., Garber, R.L., Rose, T.M., 1996. Detection and analysis of diverse herpesviral species by consensus primer PCR. *J. Clin. Microbiol.* 34, 1666–1671.
- Wellehan, J.F.X., Gagea, M., Smith, D.A., Taylor, W.M., Berhane, Y., Bienzle, D., 2003. Characterization of a herpesvirus associated with tracheitis in Gouldian finches (*Erythrura [Chloebia] gouldiae*). *J. Clin. Microbiol.* 41, 4054–4057.
- Zimmermann, L., Stephens, A., Nam, S.-Z., Rau, D., Kübler, J., Lozajic, M., Gabler, F., Söding, J., Lupas, A.N., Alva, V., 2018. A completely reimplemented MPI bioinformatics toolkit with a new HHpred server at its core. *J. Mol. Biol.* 430, 2237–2243. <https://doi.org/10.1016/j.jmb.2017.12.007>.